

a time scale of seconds, the decay of ΔF to resting levels was much slower in fast-twitch than slow-twitch fibers (average time constants of ~ 12 vs. ~ 2 s). This long tail of the Ca transient in fast-twitch fibers, which can last up to 60 s, is consistent with the large concentration of the calcium binding protein parvalbumin in EDL but not soleus fibers. Modeling of myoplasmic Ca movements in fast-twitch fibers indicates that, 1 s after an AP, most (~ 0.8) of the released Ca remains in the myoplasm where it is mainly ($\sim 95\%$) bound to parvalbumin. Ca binding by parvalbumin helps to abbreviate the Ca transient during relaxation. However, because parvalbumin brings free [Ca] close to resting levels, the modeled activity of the Ca pump is low. In consequence, Ca pumping continues for tens of seconds, as Ca is slowly returned to the sarcoplasmic reticulum. Supported by NIH and MDA.

1497-Pos Board B389

Analysis of Calcium (Ca) Transients during Excitation-Contraction Coupling in Frog Twitch Muscle Fibers

Stephen M. Baylor, Stephen Hollingworth.

University of Pennsylvania, Philadelphia, PA, USA.

Singly-dissected fibers were micro-injected with fura-2, a rapidly-responding Ca indicator. Resting fluorescence (F_R) and action-potential evoked changes (ΔF) were measured at 16°C ; $\Delta F/F_R$ was scaled to units of Δf_{CaD} , the change in fraction of fura-2 in the Ca-bound form. Measured Δf_{CaD} was compared with Δf_{CaD} simulated with a kinetic model of the underlying myoplasmic Ca movements. During the period 30-200 ms after an action potential, simulated Δf_{CaD} decayed toward baseline more slowly than measured Δf_{CaD} . If Δf_{CaD} was simulated with a modified model that incorporated competition between Mg and Ca for occupancy of the regulatory sites on troponin (assumed dissociation constant of Mg's reaction with the regulatory sites, 2.2 mM; assumed myoplasmic free [Mg], 1 mM), good agreement with measured Δf_{CaD} was observed. The results support the conclusion that Mg, at physiological levels, competes with Ca for occupancy of the regulatory sites, as indicated in some experiments from fragmented preparations, including tension-pCa measurements in skinned fibers and biochemical studies of isolated troponin molecules. Δf_{CaD} in frog was also compared with our previous measurements and simulations of Δf_{CaD} in mouse fibers (reviewed in J. Gen. Physiol., 2012). In frog, the SR Ca release flux elicited by an action potential appears to be the sum of two components. The time course of the first component is similar to that of the entire flux waveform in both fast-and slow-twitch mouse fibers, while that of the second is several-fold slower; the fractional release amounts are ~ 0.85 (first component) and ~ 0.15 (second component). An anatomical basis for two release components in frog is the presence of both junctional and parajunctional Ca release channels, whereas the mouse fibers have only junctional channels (Felder and Franzini-Armstrong, 2002). Supported by NIH (GM 086167)

1498-Pos Board B390

Myoplasmic Calcium (Ca) Movements during Relaxation and Recovery of Superfast Muscle Fibers of the Toadfish Swimbladder (TSB)

Frank E. Nelson, Stephen Hollingworth, Lawrence C. Rome, Stephen M. Baylor.

University of Pennsylvania, Philadelphia, PA, USA.

Tsb fibers produce high-frequency contractions (80-100 Hz at 16°C) that generate the fish's cyclical mating call (~ 500 ms duration, ~ 10 s intercall interval). Our aim was to understand Ca movements during the intercall interval by measuring Ca transients elicited by action potentials (APs). Fluo-4 was micro-injected into one fiber within a dissected bundle. With one AP, the peak, time of peak, and temporal half-width of $\Delta F/F_R$ (change in indicator fluorescence divided by resting fluorescence) were ~ 20 , ~ 9 ms, and ~ 14 ms, respectively. The remaining analysis considered the late time course of ΔF . From 1 to 60 s after cessation of stimulation, ΔF was well fitted by a double-exponential decay plus a small offset. With a 40-AP train at 83 Hz, the two exponential components had approximately equal amplitudes; the fast and slow time constants were ~ 2 and ~ 10 s. ΔF was well simulated with our kinetic model of Ca movements in tsb fibers (model 3; Rome et al., J. Physiol., 2011) extended to the 60 s time scale. With one AP, the estimated amount of SR Ca released is ~ 750 μM (concentration referred to the myoplasmic water volume) and $f_M(1)$ (the amount of the released Ca still in the myoplasm 1 s after cessation of stimulation) is ~ 630 μM , 97% of which is bound to parvalbumin. With 40 APs and a Ca release of ~ 5.5 mM, $f_M(1)$ is ~ 3.2 mM, with 92% bound to parvalbumin. The calling cycle thus appears to be constrained by Ca accumulation on parvalbumin and the slow rate of Ca pumping that ensues when parvalbumin lowers free [Ca] close to the resting level. Supported by NIH (GM 086167) and NSF (IOS-1145981).

1499-Pos Board B391

TRIM50 Regulates Vesicular Trafficking for Acid Secretion in Gastric Parietal Cells

Miyuki Nishi¹, Fumiyo Aoyama², Fumihiko Kisa¹, Hua Zhu³, Mingzhai Sun³, Peihui Lin³, Bo Van¹, Jianjie Ma³, Akira Sawaguchi², Hiroshi Takeshima¹.

¹Graduate School of Pharmaceutical Sciences, Kyoto, Japan, ²Faculty of Medicine, University of Miyazaki, Miyazaki, Japan, ³Department of Surgery, Davis Heart and Lung Research Institute, The Ohio State University, Columbus, OH, USA.

Within the human genome, there are ~ 80 members of the tri-partite motif (TRIM) family proteins. Our previous studies have defined MG53, a muscle-specific TRIM protein, as an essential component of the cell membrane repair machinery. Sequence homology analysis reveals a strong sequence similarity between MG53 and TRIM50 - a stomach-specific TRIM member whose biological function has yet to be defined. Our biochemical data demonstrated that TRIM50 is specifically expressed in gastric parietal cells, and predominantly localized in the tubulovesicular and canalicular membranes. In cultured cells ectopically expressing GFP-TRIM50, confocal microscopic imaging revealed dynamic movement of TRIM50-associated vesicles in a phosphoinositide 3-kinase-dependent manner. A protein overlay assay detected preferential binding of the PRY-SPRY domain from the TRIM50 C-terminal region to phosphatidylinositol species, suggesting that TRIM50 is involved in vesicular dynamics by sensing the phosphorylated state of phosphoinositol lipids. *Trim50*-knockout mice retained normal histology in the gastric mucosa but exhibited impaired secretion of gastric acid. In response to histamine, *Trim50*-knockout parietal cells generated deranged canaliculi, swollen microvilli lacking actin filaments, and excess multilamellar membrane complexes. Therefore, TRIM50 seems to play an essential role in tubulovesicular dynamics, promoting the formation of sophisticated canaliculi and microvilli during acid secretion in parietal cells.

1500-Pos Board B392

Effects of Substituting Tryptophan for Basic Residues in the S4 Voltage-Sensing Helices of $\text{Ca}_v1.1$

Roger A. Bannister, Ong Moua, Kurt G. Beam.

University of Colorado Denver-AMC, Aurora, CO, USA.

In skeletal muscle, $\text{Ca}_v1.1$ serves dual functions as the voltage sensor for excitation-contraction (EC) coupling and as an L-type Ca^{2+} channel. It has been long established that L-type Ca^{2+} current activates at potentials ~ 20 mV more depolarized than intramembrane charge movement or EC coupling. We recently characterized a $\text{Ca}_v1.1$ mutation (R174W) which affects the innermost basic residue of the voltage-sensing S4 helix of Repeat I and results in malignant hyperthermia susceptibility in humans. Interestingly, R174W abolishes activation of the L-type current in response to 200 ms depolarizations without affecting the voltage dependence of intramembrane charge movement or of SR Ca^{2+} release. In this study, we have made corresponding mutations in Repeats II (K537W), III (R906W) and IV (K1245W) and expressed these mutants in *dysgenic* ($\text{Ca}_v1.1$ null) myotubes. Confocal imaging of affixed YFP tags indicated that all the mutants were correctly targeted to membrane-SR junctions. In striking contrast to the virtual loss of channel function observed with R174W, the K537W and K1245W mutants produced enormous L-type currents with peak amplitudes nearly 8-fold greater than wild-type $\text{Ca}_v1.1$ and greatly impaired deactivation. Even though these two gain of channel function mutants activated at substantially more hyperpolarized potentials (~ 20 mV shift), the voltage-dependence of charge movement and SR Ca^{2+} release were largely unaffected. On the other hand, R906W produced currents of similar amplitude to wild-type $\text{Ca}_v1.1$ but with a consistent ~ 15 mV depolarizing shift in activation. We are currently investigating the effects of the R906W mutation on the voltage dependence of charge movement and SR Ca^{2+} release in order to determine whether RIII plays a more critical role in engaging EC coupling than the other conserved Repeats of $\text{Ca}_v1.1$. Supported by NIH AR055104 (KGB) and AG038778 (RAB), and MDA176448 (KGB).

1501-Pos Board B393

Protein Components of the Ryanodine Receptor Complex Traffic Directly from Rough ER to Concentrate in Junctional SR

Naama H. Sleiman¹, Larry R. Jones², Steven E. Cala¹.

¹Wayne State University, Detroit, MI, USA, ²Indiana University, Indianapolis, IN, USA.

Interactions of the junctional SR (jSR) proteins calsequestrin (CSQ2), triadin (TRD), and junctin (JCT) with the ryanodine receptor have been demonstrated in vitro as essential for proper SR Ca^{2+} release. However, the intracellular pathway(s) by which these critical proteins traffic to jSR sites remains unknown. To investigate pathways of trafficking for jSR proteins in adult

cardiomyocytes, wild-type canine CSQ2, TRD, and JCT were overexpressed in cultured adult rat cardiomyocytes using recombinant adenoviruses. The overexpressed proteins were detected using either species-specific antibodies, or by fusion with fluorescent proteins. After 24h and 48h, cardiomyocytes were examined using confocal fluorescence microscopy. By the time overexpressed CSQ2 was first detected by immunofluorescence (24h), it was already distributed across jSR sites. In contrast, TRD and JCT exhibited patterns of perinuclear accumulation after 24h. By 48h, they became increasingly concentrated along a transverse pathway that extended from perinuclear puncta towards the cell surface. This novel transverse jSR trafficking pathway co-localized with desmin, a prominent protein component of cardiac intermediate filaments. It was previously found that CSQ2-DsRed forms a polymeric complex that prematurely polymerizes at perinuclear sites of rough ER. We reasoned that this proximal CSQ2 polymer should then bind to newly synthesized TRD and JCT in situ, leading to their enhanced concentration around the nucleus. Indeed, when canine TRD and JCT were co-overexpressed with CSQ2-DsRed, both of these small transmembrane proteins bound to perinuclear CSQ2-DsRed, and failed to exhibit anterograde trafficking to peripheral jSR puncta. In contrast, TRD in which CSQ2 binding sites were deleted readily trafficked towards the cell periphery. Rates of anterograde trafficking of CSQ2 and other jSR proteins may depend upon the assembly of CSQ2 into polymers, which may be regulated by luminal Ca^{2+} concentrations.

1502-Pos Board B394

Calibration of Ca^{2+} Transients Obtained with the Fast Ca^{2+} and Mg^{2+} Dye Magfluor-4

Juan C. Calderon¹, Daniel Raigosa¹, Marco Giraldo¹, Pura Bolaños², Carlo Caputo².

¹University of Antioquia, Medellin, Colombia, ²Venezuelan Institute for Scientific Research, Caracas, Venezuela, Bolivarian Republic of.

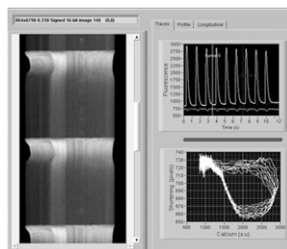
Since there are uncertainties about the concentration of free cytosolic Ca^{2+} reached in a muscle fiber during a transient elicited by electric stimulation, and about the $\text{Kd}_{\text{Ca}^{2+}}$ of the fast dye Magfluor-4, we performed two groups of experiments aimed at calibrating the Ca^{2+} transients obtained with this dye. For the fiber experiments, we used murine single skeletal muscle fibers obtained from enzymatically dissociated *flexor digitorum brevis*, loaded with 8-10 μM of the dye in its acetoxymethyl ester form, during 40 min at 21-22°C, to determine F_{max} , F_{min} and dye compartmentalization. The cells were permeabilized with saponine and exposed to 50 mM of free calcium to intracellularly saturate the dye. Compartmentalization was assessed using digitonin and triton-X100. For our conditions, F_{max} and F_{min} were 160 ± 14 ($n=9$, mean \pm SEM) and 3.4 ± 0.7 ($n=6$). Dye compartmentalization was found to be less than 10% ($n=1$). For the *in vitro* experiments, $\text{Kd}_{\text{Ca}^{2+}}$ (20°C) values of 21.6 μM , 27.8 μM and 29.1 μM were obtained in presence of 0, 1 and 2 mM free Mg^{2+} , respectively. To calculate Ca^{2+} concentration from the fluorescence signals, we used the methodologies proposed by Grynkiewicz *et al.* (1985) and by Caputo *et al.* (1994). Preliminary results, taking into account our data or some values from the literature (Baylor *et al.* 2009), show single Ca^{2+} transient's peak between 2 and 7 μM ($n=4$). We are now calculating the kinetics of Ca^{2+} transients and the quantitative changes induced by modulating Ca^{2+} release and sequestration mechanisms in different fiber types. In conclusion, we have calculated the peak Ca^{2+} concentration after single stimulation in fibers loaded with Magfluor-4. Our preliminary results are comparable to those obtained with other fast Ca^{2+} dyes, such as Magfura-5, but lower than those reported with Magfura-2.

1503-Pos Board B395

Cell Edge Detector: Recovering Length Information from Line-Scan Confocal Images

Jose L. Puglisi, Leighton T. Izu, Ye Chen-Izu, Donald M. Bers. University of California, Davis, Davis, CA, USA.

Confocal microscopy has greatly enhanced our understanding of cardiac excitation-contraction coupling. Linescan images have been used to obtain detailed information about intracellular calcium concentration disregarding the mechanical activity of the cell. In order to fill this gap we have designed an algorithm to recover the cell length information from those images. We implemented this program using LabVIEW language. An intuitive user interface allows the researcher to load the image; scan the longitudinal axis; select portion of the file; detect the borders and plot the calcium and cell shortening traces with the corresponding shortening versus calcium loop. The software also



calculates and plots into a table the following parameters: maximum fluorescence (F/F_0), decay time (τ), peak fractional shortening ($L\%$), half time to relaxation ($t_{1/2}$), maximum dL/dt , and from the loop curve the calcium concentration corresponding to half shortening (EC_{50}). This new approach allows us to obtain richer information from the linescan images by extracting the corresponding shortening traces from the fluorescence signal. This software is already operational in our labs and has been used to analyze confocal images of calcium transients and myocyte contraction in cardiac cells.

1504-Pos Board B396

TIRFM Imaging of PTRF and MG53 Translocation to Cell Surface Membrane following Osmotic-Stress Induced Injury

Hua Zhu, Ki Ho Park, Jianjie Ma.

Department of Surgery, Davis Heart and Lung Research Institute, The Ohio State University, Columbus, OH, USA.

Plasma membrane damage repair is an intrinsic physiological process for maintenance of integrity of eukaryotic cells under a variety of insults. Osmotic-shock has been widely used to induce cell membrane injury and has become a useful tool to study the mechanisms of cell membrane repair. It is known that following a series of hypo-osmotic stress, intracellular vesicles can traffic to and fuse with the cell surface membrane. These vesicles are labeled with caveolin-1 and PTRF, two essential proteins of the caveolae membrane structure. We have previously shown that PTRF can interact with MG53, a main component of the cell membrane repair machinery, for anchoring of the repair patch at the acute membrane injury site. In this study, we sought to explore the trafficking behavior of PTRF and MG53 during osmotic shock using two-color Total Internal Reflection Fluorescence Microscopy (TIRFM). We found that rapid translocation of MG53 toward the cell surface membrane could be triggered upon return of the cell to an isotonic environment following pre-exposure of the cell to a hypotonic solution (150 mOsm, 1 min). This process is PTRF dependent, as MG53 cannot translocate to cell membrane in HepG2 cells which lack endogenous PTRF expression. These data support our previous finding that PTRF is an indispensable component of the MG53-mediate membrane repair process. We are currently in the process of defining the kinetics and temporal relationship for the movement of PTRF/MG53-containing vesicles after osmotic shock, toward understanding the role for MG53/PTRF in facilitating the membrane fusion and fission processes during cell membrane repair.

1505-Pos Board B397

MG53 can Function in Keratinocyte Membrane Repair and Contribute to Excisional Wound Healing in Rodent Skin

Matthew Orange¹, Christopher Ferrante¹, Rosalie Yan², Tao Tan², Norio Takizawa², Pei-Hui Lin^{1,3}, Haichang Li³, Hiroshi Takeshima⁴, Noah Weisleder^{1,5}, Jianjie Ma^{1,3}.

¹Department of Physiology and Biophysics, UMDNJ-Robert Wood Johnson Medical School, Piscataway, NJ, USA, ²Protein Therapeutics Division, TRIM-edicine, Inc, New Brunswick, NJ, USA, ³Department of Surgery, Davis Heart and Lung Research Institute, The Ohio State University, Columbus, OH, USA, ⁴Department of Biological Chemistry, Kyoto University, Kyoto, Japan, ⁵Department of Physiology and Cell Biology, Davis Heart and Lung Research Institute, The Ohio State University, Columbus, OH, USA.

Plasma membrane repair is a dynamic cellular process observed in many cell types where membrane disruptions are actively repaired by a vesicle-mediated mechanism. Mitsuguimin 53 (MG53) is a novel member of tripartite motif (TRIM) family of proteins and an important component of the membrane repair machinery. In skeletal muscle, MG53 protects against eccentric contraction related damage while in cardiac muscle, MG53 protects against ischemia-reperfusion injury. While previous studies illustrate MG53 function in striated muscles, little is known about MG53 function in other tissues. The skin is an organ that covers the entire body and is constantly exposed to various environmental factors that can induce membrane disruptions. Here we investigated the function of MG53 in the skin and its contribution to wound healing. The presence of extracellular recombinant human MG53 (rhMG53) protected primary human keratinocytes from mechanical damage. Expression of GFP-MG53 in cultured human keratinocytes confirmed that the protein responded to membrane damage in the same fashion as in muscle fibers and other non-muscle cells. Excisional wounding revealed delayed healing of *mg53*^{-/-} mice when compared to wild-type. While western blotting showed MG53 expression in extracts of mouse skin, MG53 was not expressed in human or mouse cultured keratinocytes. Immunohistochemistry revealed that expression of MG53 in mouse skin was specific to the panniculus carnosus, a subdermal striated muscle layer common in rodents that has limited distribution in human skin. Together these data suggest that MG53 has potential as a therapeutic agent to increase wound healing in a variety of tissues.